KINETIC CHARACTERISTICS OF SPALL FRACTURE

A. N. Dremin and A. M. Molodets

UDC 539.4.019.1

The fracture process that occurs during interaction of opposing rarefaction waves is called spall. The whole process hence proceeds within $\sim 10^{-6}$ sec, which is 3-5 orders of magnitude lower than for quasistatic fracture, and the maximum negative stress (spall strength) is correspondingly several times greater.

Up to now it has been established that the time of negative stress action during spall, together with the stress itself, plays an important part [1, 2], while the question of separating the spall fracture process into stages, just as is done in investigations of quasistatic fracture [3, 4], is discussed to some degree in practically every paper on spall.

Thus, the initial stage of spall fracture is considered in [5] as the process of generation and growth, whereupon microcracks appear and grow, and satisfactory agreement is obtained with experiment for moderate damage levels in the metals. This same approach is used in [6] in an investigation of spall in a polycarbonate. In this paper it is proposed to consider four spall fracture stages. In [7] it is proposed to consider two spall stages. It is also recommended to describe spall as a two-stage process in [8]. The need to delimit the spall fracture process is also mentioned in [9, 10].

Therefore, delimiting the spalling process by stages can be considered standard; however, the question of the quantity of stages, and therefore, of their characteristics and conditions for making the transition from one stage to another remains open.

Moreover, despite the fact that schemes for the time dependences used for the spall strength permit the mutual matching of data on spalling [7-15], such dependences (see [15], say) do not allow extrapolation into the large loading time domains ($\sim 10^{-3}$ sec). The question of the correlation between spall and quasistatic data is discussed in the literature in [5, 7, 8, 15, 16].

The spall process is delimited into pre- and postcritical stages in this paper, in the sense of the definition given for the stages in [4], a description of the precritical spalling fracture stage in metals is proposed, and the correlation between spalling and quasistatic strength measurements is also established.

The results of recording the free surface velocity in steel by a capacitive transducer method [17] under the conditions of one-dimensional loading in three series of experiments with a substantially different stress profile shape in the passing compression wave were the initial experimental data.

The stress profile shape in specimens at the distance of the free surface from the plane of shock-wave entry was verified by using manganin pressure transducers [18]. The shock amplitude σ_0 was here for 90 kbar, for the first series, the stress profile behind its front had a descending shape with a characteristic 6-μsec duration. The second series, σ_0 = 105-120 kbar, is characterized by a 2-μsec pulse duration for a shape similar to the pulse shape in the first series. In the third series σ_0 was 130 kbar and the wave profile was almost rectangular with a 2-μsec duration.

The steel St. 3 specimens of 120-mm diameter were cut perpendicularly to the axis from a bar as delivered. From handbook data [19], St. 3 with a 0.18% carbon content has a strength σ_B = 4 kbar at a temperature T = 293°K, a yield point σ_τ = 2.4 kbar, and a Young's modulus E = 2020 kbar.

Experimental oscillograms of the current in the capacitive transducer loop are presented in Figs. 1a-c for a recording of the free surface velocity during spall in the first, second, and third series, respectively (*a* is 1 μsec/division, b and c are 0.5 μsec/division). A section of the free surface velocity profile, obtained after processing the oscillogram in Fig. 1b, is shown in Fig. 2. The cross denotes the error, and the time origin is the time of emergence of the elastic precursor on the free surface.

Represented in Fig. 3a is the diagram of the free surface profile W(t) under spall that is characteristic for this paper. The following quantities were determined from the experimental profiles: the maximum velocity W_A at the time t_A, the minimum velocity W_B at the time t_B, the acceleration W'_+ in the left neighborhood of t_B (the dashed line in the profile of Fig. 3a), the acceleration W'_+ in the right neighborhood of t_B, the time between the nearest minimums of the velocity t_2, t_3, t_4, and the time $t_1 = t_B - t_A$. In the third series the time was measured from the time of emergence of the steepest section of the plastic wave onto the free surface. The small strength σ^* was determined by the formula $\sigma^* = 0{,}5c_0\rho_0\Delta W^*$

Chernogolovka. Translated from Zhurnal Prikladnoi Mekhaniki i Tekhnicheskoi Fiziki, No. 6, pp. 85-95, November-December, 1980. Original article submitted November 29, 1979.

0021-8944/80/2106-0806$07.50

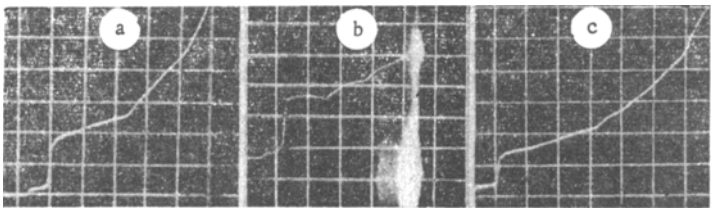

Fig. 1

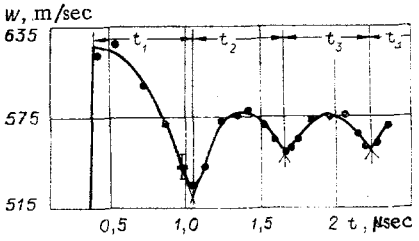

Fig. 2

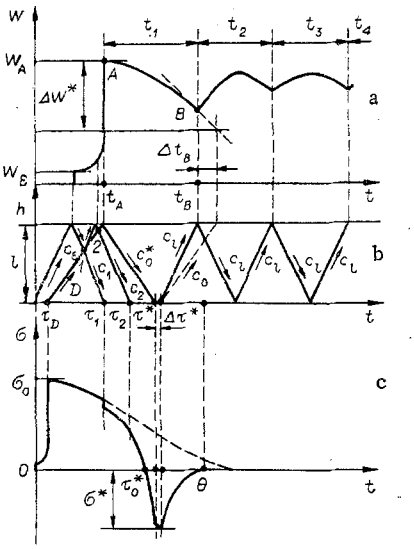

Fig. 3

[20] in the first and second series, with a correction for the elastic-plastic behavior of the material $\Delta W^* = W_A - (W_B + W'\Delta t_B)$[21], where $\Delta t_B = 0.5t_2 (c_l/c_0 - 1)$ [21, 22]. In the formulas for σ^* in St. 3, the density of the material was ρ_0 = 7.86 g/cm^3, the bulk speed of sound was c_0 = 4.64 km/sec, and the longitudinal speed of sound in St. 3 is c_l = 5.95 km/sec [22]. Determination of σ^* in the experiments in the third series was difficult because of the great steepness of the graph of W(T) to the left of the point B in this series. Specular spalling [23] was realized in the third series.

The velocity fluctuations with period t_2 that follow the point B indicate that a second free surface, or a domain with low dynamic stiffness, appears at a distance $l = 0.5t_2c_l$ [22] from the free surface within the specimen.

The values of t_1, t_2, l, σ^*, as well as of the ratio between the times t_1/t_2 are presented in Table 1 for individual tests of each series.

Investigation of the specimens conserved after spalling [5, 6] discloses a set of cracks of different size. Description of the behavior of such a discontinuous material in the terms of the mechanics of a continuous medium is related to the introduction of complex [5] models. However, separation of the specimen into a sufficiently thin layer occurs during spall in many cases, i.e., the size of the roughness on the spalling fracture surfaces is several times less than the thickness of the spalling plate. This affords the possibility of considering the spalling process in just this layer.

A metallographic study of the specimens conserved in tests corresponding to Fig. 1 permits the exposure of a strong damage layer of thickness $2\Delta l_1$, whose core is at a distance l_1 from the free surface. Values of l_1 and Δl_1 are presented in Table 1.

It is seen from Table 1 that $\Delta l_1 \leqslant (0.15 - 0.01)l_1$ and l_1 practically agrees with l. In this connection, let us examine spall within the framework of the following scheme.

Let us define the spall plane as a layer of thickness δ, whose middle is at a distance l from the free surface, where $l \gg \delta$, and a material that remains monolithic during the whole spall process abuts on the boundary of this layer. The boundary of the layer turned toward the free surface is denoted by δ_+ and the opposite by δ_-. For a sufficient smallness of δ the stresses at δ_+ and δ_- differ slightly, remaining practically identical even for a certain time after the beginning of fracture in this layer. Hence, we will understand stress in the layer to be stress on δ_+ for the requisite smallness of δ. Since the boundaries belong to a monolithic material, the stresses on the boundaries are related to their velocities by the equation of state of a monolithic material, independently of the processes going on within the layer. During fracture, the law of stress variation with time on the boundary δ_+ will govern the change in free surface velocity.

TABLE 1

Series No.	$t_1 \pm 3\%$, μsec	$t_2 \pm 3\%$, μsec	$(t_1/t_2) \pm 6\%$	$\Delta\tau^*$, μsec	σ^*, kbar	l, mm	$l_1 \pm \Delta l_1$, mm
1	2,18	1,82	1,198	+0,05	16	5,4	5,5±0,5
2	0,66	0,59	1,119	−0,02	27	1,7	1,6±0,2
3	1,58	1,38	1,145	−0,003	—	4,14	4,1±0,05

The description of spall within the scheme accepted reduces to setting up a law of expansion of the fracturing layer. The process of growth of discontinuities in the spall plane is developed continuously most often [24]. However, by analyzing the change in the free surface velocity during spall, a certain characteristic time can be extracted in this process. Acceleration of the free surface (see Fig. 2) changes the sign in a small ($\sim 0.10 t_2$) neighborhood of t_B, being changed here by $(W'_+ - W'_-)$, which is $(2\text{-}8)\cdot 10^8$ m/sec^2, i.e., in practice the acceleration at the point B experience a jump. At some time the boundary δ_+ would also experience a jump in acceleration of the same order; from symmetry considerations the boundary δ_- would be accelerated in the opposite direction. Therefore, an especially abrupt (intense) expansion (fracture) of the layer δ starts at a certain time.

By comparing the times t_1 and t_2, the time of the beginning of intensive fracture in the spall plane can be set with sufficient accuracy. Experiments showed that despite the fact that the spall strength in the first series is 1.5 times less than in the second, while the times t_1 and t_2 are correspondingly three times greater, the ratio t_1/t_2 of the times in each series remains constant (see Table 1). This means that intensive fracture starts in the spall plane practically immediately after the passage of the tension wave front, and therefore, preparation to intensive fracture occurs, at least, in the tension wave front. In conformity with this assertion, we construct a gasdynamic scheme for spall (see Figs. 3a-c; the measuring time is the same for both).

In order to construct the dependence $\sigma(t)$ of the stress σ on the time t in the spall plane, we first consider Fig. 3b, which is an h−t diagram (h is a one-dimensional Lagrange coordinate) illustrating propagation of perturbations in the near-surface layer of a specimen of thickness l. The trajectories of those perturbations whose emergence (entrance) at the free surface or in the spall plane is indicated in the form of characteristic points on the profile W(t) or $\sigma(t)$ are shown by lines in the h−t plane. Arrows near the lines show the direction of propagation of the perturbations, and the letters denote the velocities along the lines. These same letters are also a designation of the corresponding perturbations. The elastic precursor c_ϵ with amplitude $\sigma_\varepsilon \simeq 0.5 W_\varepsilon c_l \rho_0$, which is reflected from the free surface, interacts with the lagging plastic wave D of amplitude σ_0 at the point 1. Consequently, an elastic rarefaction wave with amplitude $\leqslant \sigma_\varepsilon$ proceeds deep into the specimen from the point 1 along the compressed substance, and a compression wave whose elastic part will have the velocity c_l will proceed to the free surface. The process is repeated at the point 2, and afterwards a rarefaction wave with the total amplitude $\leqslant 2\sigma_\varepsilon$ proceeds into the specimen bulk. An estimate of the amplitude of the rarefaction wave follows from an examination of the process in the σ−u diagram, where u is the mass flow rate (see [21], for instance). As a result of multiple interactions analogous to interaction at the point 1, an elastic-plastic rarefaction wave will be introduced into the specimen up to the time t_A. The domain enclosed by this wave is included between the lines c_1 and c_0^* in Fig. 3b. As follows from the results in [25], a decrease in the perturbation propagation velocity as the pressure drops will occur continuously in the elastic-plastic unloading wave. In this connection, we assume that the perturbation propagation velocities will decrease smoothly in the elastic-plastic unloading wave even for steel as the pressure diminishes. According to our data, the first perturbation of the elastic-plastic rarefaction wave in steel has a Lagrange velocity of 6.5 km/sec at a 100-kbar pressure. Since spalling occurs in the domain of comparatively moderate negative pressures 30-40 kbar, c_0^* does not differ radically from c_0, the bulk speed of sound at zero pressure. On the basis of the above, we assume $c_2 = c_l$, $c_0^* = c_0$.

Knowledge of these velocities permits a more accurate determination of the time of the beginning of the intensive fracture in the spall plane. Let intensive fracture occur at a time $\Delta\tau^*$ after the arrival of c_0^* in the spall plane. Perturbations will proceed on both sides of the spall plane. The first small perturbation from the boundary δ_+ will traverse the distance l with the velocity c_l, be reflected from the free surface at the time t_B, and will then circulate between the free surface and the spall plane. On the basis of Figs. 3a, b we write the equation $t_B - t_A = l/c_0^* + l/c_l + \Delta\tau^*$. Substituting the expression for $l = 0.5 t_2 c_l$ into this equality we obtain

$$\Delta\tau^*/t_2 = t_1/t_2 - 0.5\,(c_l/c_0^* - 1). \qquad (1)$$

Results of estimating $\Delta\tau^*$ by means of (1) for values of $c_0^* = c_0 = 4.64$ km/sec and $c_l = 5.95$ km/sec are presented in Table 1 for appropriate tests in each series. The possibility of using the velocities c_0 and c_l in (1) was verified by tests with artificial spall for steel St. 3 performed in an apparatus identical to the test formulation in the second series [22]. Let us note that although the error in estimating $\Delta\tau^*$ is $\sim 100\%$, it can nevertheless be said that the quantity $\Delta\tau^*$ is a small quantity, less than the spread in the elastic-plastic rarefaction wave leaving the free surface, estimated as $\tau^* - \tau_2 = l/c_0 - l/c_l$.

Let us construct the stress profile in the spall plane. At the time t = 0 (see Figs. 3b, c), an elastic precursor passes through the spall plane (as yet monolithic), and a plastic wave $\sigma(\tau_D) = \sigma_0$ at the time τ_D. A passing rarefaction wave enters

the spall plane at the time τ_D. If the specimen were infinite in size in the propagation direction of this wave, then the dependence $\sigma(t)$ would govern the profile of the passing unloading wave shown in Fig. 3c by the solid line between τ_D and τ_1 and the dashed line for $t > \tau_1$. But since the first perturbation of the elastic-plastic rarefaction wave from the free surface arrives at the spall plane at the time τ_1, then starting from this time the profile $\sigma(t)$ is determined by the superposition of these waves. The result of superposing these waves in conformity with Fig. 3b is shown in Fig. 3c by the solid line in the section $\tau_1 \leqslant t \leqslant \tau^* + \Delta\tau^*$. Starting with the time $\tau^* + \Delta\tau^*$, the dependence $\sigma(t)$ is determined substantially by the intensive fracture which has started in the spall plane. Analyzing the perturbation propagation in the specimen between the free surface and the boundary δ_+ in $\sigma - u$ coordinates during fracture in an acoustic approximation, and taking into account the nature of the experimental profile W(t) for the time t_B (see Fig. 3a), a law for stress variation on the boundary δ_+ can be set up experimentally, i.e., in the spall plane. In conformity with Figs. 3a, b, the continuous curve in Fig. 3c from the time $\tau^* + \Delta\tau^*$ to the time of final separation of the specimen θ displays the section of the profile $\sigma(t)$ in the spall plane under intensive fracture.

Thus, the stress profile in the spall plane is exhibited in Fig. 3c by the solid curve. The section $\sigma(t)$ for $\tau_0^* \leqslant t \leqslant \tau^*$ will be called the tension wave front. The negative part of $\sigma(t)$ from the time τ_0^*, when $\sigma(\tau_0^*) = 0$ to the time θ when $\sigma(\theta) = 0$ in Fig. 3c is similar to the "tension stress diagram" examined in [7, 14, 26]. However, it should be noted that in constructing the negative part of $\sigma(t)$, it is essential in Fig. 3c that the tension wave front duration $\tau^* - \tau_0^*$ increases as the rarefaction wave is propagated from the free surface into the bulk of the specimen. The time $\tau^* - \tau_0^*$ in the spall coordinate will depend also on the fact what the passing compression pulse front would be (see [16], say). But even in the case of a passing shock, the duration of the tension wave front will have a finite value. This quantity is determined by the thickness of the spall plate at the site of spall.

Let us make an analogy between fracture in the spall plane and the fracture scheme used under quasistatic conditions. Using the terminology in [4], we extract the subcritical stage as a cumulative damage process proceeding to the time $\tau^* + \Delta\tau^*$ when $\sigma(t) = \sigma^*$ is the critical state characterized by the spall strength σ^* during spall fracture (see Fig. 3c) and the post-critical state proceeding from the time $\tau^* + \Delta\tau^*$ to the time θ when $\sigma(\theta) = 0$.

Let us examine quantitatively the subcritical spall state. Let us associate the beginning of the subcritical stage (see Fig. 3c) with the time of negative stress appearance in the spall plane τ_0^*, and termination because of the smallness of $\Delta\tau^* - c$ with the time τ^*, i.e., let us assume that the main quantity of embryonic damage is formed for a negative stress and high strain rate. This assumption is in agreement with the situation that plastic strain [27] plays a large part in the formation of embryonic defects.

To describe the subcritical stage we use the damage function φ and the expression for its growth rate [28]

$$\frac{d\varphi}{dt} = A(\sigma)^{m-1}, \tag{2}$$

where σ is the tensile stress, A, m are constants, t is the time, and φ is a scalar equal to 0 at the beginning of the subcritical stage, and 1 at its end.

Let σ be $\sigma(t)$ in (2), where $\tau_0^* \leqslant t \leqslant \tau^*$ (see Fig. 3), then $\varphi(\sigma(\tau_0^*)) = 0$, and the condition for the onset of the post-critical stage is $\varphi(\sigma(\tau^*)) = 1$. Since $\delta \ll l$, then the time for acoustic wave passage of the layer δ, which equals $\sim\delta/c_l$, is several times less than the action time of the unloading wave from the free surface, that equals $\sim l(1/c_0 - 1/c_l)$. We consequently assume that the condition $\varphi = 1$ in the spall plane is satisfied simultaneously in the whole layer δ.

Let us represent the shape of the tensile wave front by the line

$$\frac{d\sigma}{dt} = \rho_0 c_0^2 \varepsilon' = \text{const}, \tag{3}$$

where σ, t is the same as in (2), and ϵ' is the strain rate. The tensile stress $\sigma(t)$ in (2), (3) and henceforth is assumed positive.

Dividing (2) by (3) and integrating the expression obtained with respect to σ while taking into account that $\varphi(0) = 0$ and $\varphi(\sigma^*) = 1$, and then taking the logarithm of the result of the integration, we obtain

$$\lg \sigma^* = m^{-1} \lg \varepsilon' + m^{-1} \lg (\rho_0 c_0^2 m/A), \tag{4}$$

which is the criterion interrelating the spall strength and the constant plastic strain rate ϵ' during tension. As a first approximation we take $\varepsilon' = \varepsilon_1' + \varepsilon_2'$, where $\varepsilon_1' = 0.5 W_A'/c_0 l(1/c_0 - 1/c_l)$ is the contribution in the strain rate introduced by the rarefaction wave from the free surface, and $\varepsilon_2' = -0.5 W_-'/c_0$ is the contribution to the strain rate from the passing unloading wave.

The experiment results in the first (points I) and second (points II) series are represented in Fig. 4 in conformity with (4). The line 1 is drawn through the experimental points by the method of least squares.

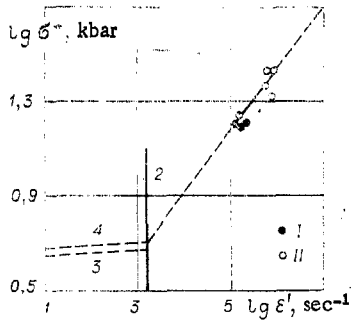

Fig. 4

Thus, a dependence is obtained for the critical characteristic, the spalling strength on the strain rate in the subcritical stage of spalling fracture. This dependence [see (4)] can be considered as the analog of the dependence of the creep strength σ_c on the rate of steady creep v' or of durability τ_p on σ_c.

On the basis of [29]

$$v' = v_0' \exp((U_0 + \gamma\sigma_c)/kT); \quad (5)$$

$$\tau_p = \tau_0 \exp((U_0 - \gamma\sigma_c)/kT); \quad (6)$$

$$\tau_p v' = v_0 = \text{const}, \quad (7)$$

where k is the Boltzmann constant, T is the absolute temperature, and v_0', τ_0, U_0, γ, v_0 are constants. Since the quantity v_0 depends slightly on the stress and the temperature, then [30]

$$v'(\sigma_c, T) = v_0/\tau_p(\sigma_c, T). \quad (8)$$

Before proceeding to a comparison between the dependence of the spalling and quasistatic strengths on the strain rate, let us make two remarks.

A state is considered quasiequilibrium in ordinary mechanical tests if the elastic waves succeed in passing through the specimen before termination of the loading. The working part of the specimen was $d \approx 2\cdot10^{-2}$ m [30] in the determination of the time dependence of the strength. Therefore, the equilibrium condition is satisfied $\tau_p \gg d/c$, since the time the elastic wave passes the specimen at the speed of sound in rods $c = (E/\rho_0)^{1/2} \approx 5\cdot10^3$ m/sec characteristic for solid is $\tau_p \gtrsim 10^{-3}$ sec [30]. However, extrapolation of the experimental results obtained for the quasiequilibrium state outside this boundary is generally not legitimate. At the same time, the spalling data should agree with the quasistatic data in the domain where the quasistatic data are known to be valid. In this connection, let us define the boundary of quasistatic data extrapolation over the time of the process as τ_Γ = d/c or, by using the relationship (7) between τ_p and v', we define this boundary by means of the strain rate as

$$v_\Gamma' = v_0 c/d. \quad (9)$$

For many materials $v_0 \sim 0.1$ [31], from which $v_\Gamma' = 10^4\,\text{sec}^{-1}$ to the accuracy of an order. For iron with the values $v_0 = 10^{-2.2}$ [32], E = 2020 kbar, $\rho_0 = 7.86$ g/cm³, $d = 2\cdot10^{-2}$ m, we obtain $v_\Gamma' = 2.59\cdot10^{2.8}$ sec⁻¹. The graph of $\lg v_\Gamma' = \text{const}$ for iron is shown by the line 2 in Fig. 4.

The temperature of iron after shock compression to 130 kbar and subsequent unloading is 303°K [33]. Since spalling occurs under tension, the mean temperature of the material was hence still less in our experiments. Hence, in comparing the spall and quasistatic data, we use the results of quasistatic measurement at room or at almost room temperature.

The creep and durability of technical iron with 0.1% carbon and $\sigma_в = 3.56$ kbar, $\sigma_\tau = 2.08$ kbar, i.e., iron whose characteristics differ negligibly from the analogous characteristics for St. 3, were investigated in [34]. The time dependence of the strength being observed at T_1 = 233°K and T_2 = 198°K is missing for T_3 = 291°K [34], which is explained by strain aging [35, 34]. For higher strain rates the time dependence of the strength of technical iron is manifest even at room temperature [35].

The continuation of the temperature-time dependence of the strength of technical iron from [34] is represented in Fig. 4 in the coordinates $\lg\sigma_c = \ln\sigma^*$, $\lg v' = \lg\varepsilon'$, where curve 3 is for T_1 and curve 4 for T_2. The transfer of the dependence $\tau_p(\sigma_c, T)$ [34] into $v'(\sigma_c, T)$ is accomplished by means of (8) by using $v_0 = 10^{-2.2}$ for iron from [32]. It is

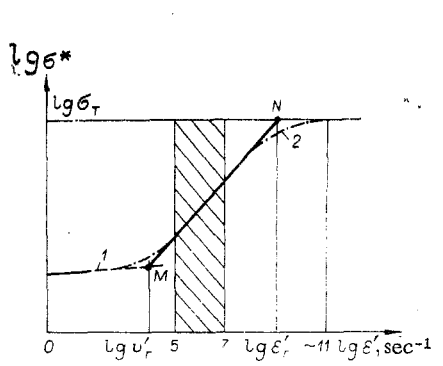

Fig. 5

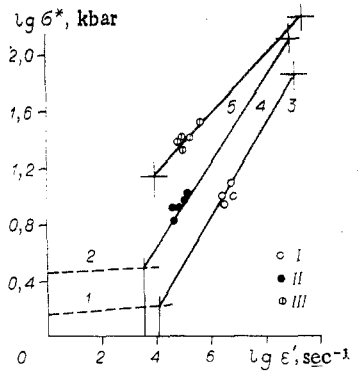

Fig. 6

TABLE 2

Metal	T, °K	U_0, kcal/mol.	γ, $\frac{mm^2 \cdot kcal}{kg \cdot mol.}$	τ_0, sec	ν_0	E, kbar	G, kbar	K, kbar	ρ_0, g/cm³
Al	293	53 [30]	2,6 [30]	10^{-13} [30]	$10^{-1,3}$ [32]	719 [39]	272 [39]	746 [39]	2,785 [40]
Cu	293	81 [30]	2,3 [30]	10^{-13} [30]	$10^{-1,7}$ [32]	1250 [39]	464 [39]	1420 [39]	8,9
U	293	—	—	—	—	1050—1750 [38]	880 [41]	—	19,04 [41]

Note: G is the shear modulus, and K the volume modulus. In addition to the value of the quantity, the paper from which the number was taken is mentioned.

seen from Fig. 4 that extrapolation of the time dependence of the strength (curves 3 and 4) and the dependence of the spall strength on the strain rate (line 1) to the boundary of the quasistatic domain (line 2) results in reasonable agreement between the dependences.

It is known that dislocations [36] play a large part in the formation of embryonic cracks in metals. In this connection it can be expected that a value for the spall strength of a material almost without defects, i.e., commensurate with the theoretical strength, will be realized for a subcritical spall fracture stage duration commensurate with the buildup time $\Delta\tau$ of a stationary velocity of dislocation motion. By using (4) with the coefficients found for the steel St. 3, we estimate the spall strength σ_T^* at small times. The buildup time for the stationary dislocation velocity is estimated by the quantity $\Delta\tau = 7 \cdot 10^{-12}$ sec [37]. Having taken the time of the subcritical stage $\Delta\tau_T = \tau^* - \tau_0^* = 7 \cdot 10^{-11}$ sec, which is not much greater than the time $\Delta\tau$, and estimating the strain rate here as $\varepsilon_T' = \sigma_T^*/\rho_0 c_0^2 \Delta\tau_T$, we obtain $\sigma_T^* = 193$ kbar by using (4). This value is close to the estimate of the theoretical strength 200 kbar from the formula $\sigma_T = 0.1E$ [28], where E is the Young's modulus for steel.

Therefore, the correlation between the dependence of the spalling strength on the strain rate and the time dependence of the strength in quasistatic tests and the estimates of the theoretical strength justifies the reasonableness of the assumptions made in this paper to describe the subcritical stage of spall fracture.

In this connection, a role can be proposed for estimating the dependence of the spalling strength on the strain rate in the range 10^5-10^7 sec^{-1} under the assumption that (2) is valid even for other metals. This rule is illustrated in Fig. 5, where curve 1 is the continuation of experimental data on durability in the domain of high strain rates. The ordinate of the point M is determined by the intersection of curve 1 with the boundary of extrapolation of the quasistatic data, defined by using (9) as $\lg \varepsilon' = \lg v_r' = \text{const}$, where the coordinates of the point N are $\lg \sigma^* = \lg \sigma_T$ and $\lg \varepsilon' = \lg \varepsilon_T'$, where $\sigma_T = 0.1$ E, $\varepsilon_T' = \sigma_T/\rho_0 c_0^2 \Delta\tau_T$. The section of the line MN lying in the shaded domain will yield the desired dependence of the spalling strength on the strain rate.

The lines constructed in this manner for Al, Cu, U (lines 3-5, respectively) are shown in Fig. 6. The quantities used here are presented in Table 2. Curves 1 and 2 are the time dependence of the strength for Al and Cu, respectively. Because of the absence of data on the durability of uranium, the value 10^4 sec^{-1} is taken as v_r' for this metal, and the maximum value $\sigma_B = 3.7$—14kbar [38] is taken as the ordinate of the point corresponding to the ordinate of the point M in Fig. 5. The quantity $\Delta\tau_T$ was assumed identical ($7 \cdot 10^{-11}$ sec) for all metals.

The results of processing literature data on spall are also represented in Fig. 6. In conformity with Fig. 3a in this paper, graphs of the free-surface velocity presented in Fig. 2 from [40] for Al and analogous data for uranium presented in Figs. 10c, 10d, 11a, 11b, and 12a from [41] were processed. Experiments on the collision of plates [1] presented in [11] were used for Cu. Tests with the same minimal thickness of the impactor were selected from each group of tests [1] with constant collision velocity, where only the embryonic spall was recorded in this group starting from this minimal thickness. It is considered that the fracture in [1] is concentrated in a target of thickness h_2 at a depth of impactor thickness h_1 from the free target surface. The steep slope of the tension wave front at this was was estimated as $\tau^* - \tau_0^* = (1/c_0 - 1/c_l)/(1/h_1 + 1/h_2)$ (this relationship follows from the examination of the h–t diagram for plate collisions), and the strain rate in the subcritical stage as $\varepsilon' = \sigma^*/\rho_0 c_0^2 (\tau^* - \tau_0^*)$ correspondingly. The velocities c_0 and c_l for all three metals were computed by the formulas $c_0 = (K/\rho_0)^{1/2}$, $c_l = ((K + 4G/3)/\rho_0)^{1/2}$, where the values of K and G were taken at zero pressure. The I in Fig. 6 are experimental points for Al according to data in [40], the II are for Cu from data in [1], and III are for U from data in [41].

It is seen in Fig. 6 that the experimental points are grouped around the predicted dependences, and deviated by not more than 20% in σ^*, which is no worse than the accuracy of the majority of measurements of the spall strength. For instance, the accuracy in determining σ^* in [20] is 30%. The dependence of the spall strength of metals on the strain rate apparently has the form of the curve 2 (see Fig. 5). For strain rates in the area of v'_Γ this dependence goes smoothly over into the experimental data on durability. The inertia of the dislocations becomes substantial in the domain of ϵ'_Γ, and hence, the spall strength depends to a lesser degree on the strain rate, approaching the theoretical value.

Therefore, the separation proposed in this paper for spalling fracture into sub- and postcritical stages permits giving a quantitative description, in a first approximation, for the dependence of the spall strength on the strain rate, which agrees with the time dependence of the strength under quasistatic fracture.

LITERATURE CITED

1. J. H. Smith, "Three low-pressure spall thresholds in copper," in: Dynamic Behavior of Materials, ASTM, Philadelphia (1963).
2. D. W. Blinkow and D. V. Keller, "Experiments on the mechanism of spall," in: Dynamic Behavior of Materials, ASTM, Philadelphia (1963).
3. G. T. Khan, B. L. Averbach, W. S. Owen, and M. Cohen, "Origin of chip microcracks in polycrystalline iron and steel," in: Atomic Mechanism of Fracture [in Russian], Metallurgizdat, Moscow (1963).
4. Ya. B. Fridman, Mechanical Properties of Metals [in Russian], Pt. 1, 3rd edn., Mashinostroenie (Moscow).
5. T. W. Barbee, L. Seamon, R. Grewdson, and D. Curran, "Dynamic fracture criteria for ductile and brittle metals," J. Mater., 7, No. 3 (1972).
6. D. R. Curran and D. A. Shockey, "Dynamic fracture criteria for a polycarbonate," J. Appl. Phys., 44, No. 9 (1973).
7. N. A. Zlatin, G. S. Pugachev, S. M. Mochalov, and A. M. Bratov, "Time dependence of the strength of metals for microsecond band longevities," Fiz. Tverd. Tela, 17, No. 9 (1975).
8. A. G. Ivanov and V. N. Mineev, "On the scaling criterion for brittle fracture of a structure," Dokl. Akad. Nauk SSSR, 220, No. 3 (1975).
9. V. S. Nikiforovskii, "On the kinetic nature of brittle fracture of solids," Zh. Prikl. Mekh. Tekh. Fiz., No. 5 (1976).
10. Yu. I. Fadeenko, "Time criterion of fracture by explosion," Zh. Prikl. Mekh. Tekh. Fiz., No. 6 (1977).
11. B. M. Butcher, L. M. Barker, D. E. Munson, and C. D. Lundergan, "Influence of stress history on time-dependence in metals," AIAA J., 2, No. 6 (1964).
12. F. R. Tuler and B. M. Butcher, "A criterion for the time dependence of dynamic fracture," Int. J. Fract. Mech., 4, No. 4 (1968).
13. L. J. Cohen and H. M. Berkowitz, "Time-dependence fracture criteria for 6061-T6 aluminum under stress-wave loading in uniaxial strain," Int. J. Fract. Mech., 7, No. 2 (1971).
14. N. A. Zlatin, S. M. Mochalov, G. S. Pugachev, and A. M. Bragov, "Time regularities of metal fracture under intensive loads," Fiz. Tverd. Tela, 16, No. 6 (1974).
15. B. A. Tarasov, "On the time-dependence of the strength of organic glass under shock loading," Probl. Prochn., No. 2 (1972).
16. L. D. Volovets, N. A. Zlatin, and G. S. Pugachev, "On the fracture mechanism of solids in microsecond band lifetimes," Pis'ma Zh. Tekh. Fiz., 4, No. 18 (1978).
17. A. G. Ivanov and S. A. Novikov, "Capacitive transducer method for recording the instantaneous velocity of a moving surface," Prib. Tekh. Eksp., No. 1 (1963).
18. G. I. Kanel', "Application of manganin transducers to measure the shock compression pressure of condensed media," [in Russian], VINITI, No. 477-74 dep. (1974).
19. E. P. Mogilevskii, Materials in Machine Construction [in Russian], Vol. 2, Mashinostroenie, Moscow (1967).
20. S. A. Novikov, I. I. Divnov, and A. G. Ivanov, "Investigations of the fracture of steel, aluminum, and copper under explosive loading," Fiz. Metl. Metalloved., 21, No. 4 (1966).
21. G. V. Stepanov, "Spall fracture of metals by plane elastic-plastic waves," Probl. Prochn., No. 8 (1976).
22. A. M. Molodets, "Measurement of the spall strength in three steels," in: Detonation, Critical Phenomena. Physico-chemical Transformations in Shocks [in Russian], Chernogolovka (1978).

23. A. G. Ivanov and S. A. Novikov, "On rarefaction shocks in iron and steel," Zh. Eksp. Teor. Fiz., 40, No. 6 (1961).
24. L. Davison and A. S. Stevens, "Continuum measure of spall damage," J. Appl. Phys., 43, No. 3 (1972).
25. A. N. Dremin and G. I. Kanel', "Compression and rarefaction waves in shock-compressed metals," Zh. Prikl. Mekh. Tekh. Fiz., No. 2 (1976).
26. L. D. Volovets, N. A. Zlatin, and G. S. Pugachev, "Origin and development of submicrocracks in polymethylmethacrylate under dynamic tension (spall)," Pis'ma Zh. Tekh. Fiz., 4, No. 18 (1978).
27. A. V. Stepanov, Principles of the Practical Strength of Crystals [in Russian], Nauka, Moscow (1974).
28. L. M. Kachanov, Principles of Fracture Mechanics [in Russian], Nauka, Moscow (1974).
29. S. N. Zhurkov and T. P. Sanfirova, "Relation between strength and creep of metals and alloys," Zh. Tekh. Fiz., 28, No. 8 (1958).
30. V. R. Regel', A. I. Slutsker, and É. E. Tomashevskii, Kinetic Nature of the Strength of Solids [in Russian], Nauka, Moscow (1974).
31. V. R. Regel', A. I. Slutsker, and É. E. Tomashevskii, "Kinetic nature of the strength of solids," Usp. Fiz. Nauk, 106, No. 2 (1972).
32. B. Ya. Pines and A. F. Sirenko, "On the question of the correlation between the creep rate and longevity under load in metals," Fiz. Met. Metalloved, 10, No. 3 (1960).
33. R. G. McQueen and S. P. Marsh, "Equations of state for nineteen metallic elements from shock wave measurements," J. Appl. Phys., 31, No. 7 (1960).
34. L. S. Moroz, Yu. D. Khesin, and T. K. Marinets, "Investigation of creep and creep strength of iron at low temperatures," Fiz. Met. Metalloved., 13, No. 6 (1962).
35. B. M. Rovinskii and L. M. Rybakova, "Time dependence of strength under active loading," Fiz. Met.. Metalloved., 9, No. 4 (1960).
36. A. H. Cottrell, "Theoretical aspects of the fracture process," in: Atomic Mechanism of Fracture [in Russian], Metallurgizdat, Moscow (1963).
37. J. J. Gilman, "Dislocation dynamics and the response of materials to impact," Appl. Mech. Rev., 21, No. 8 (1968).
38. A. N. Zelikman, Metallurgy of Rare-Earth Metals Thorium and Uranium [in Russian], Metallurgizdat, Moscow (1970).
39. M. L. Bernshtein and V. A. Zaimovskii, Structure and Mechanical Properties of Metals [in Russian], Metallurgizdat, Moscow (1970).
40. C. S. Specht, P. F. Taylor, and A. A. Wallag, "Observation of spallation and attenuation effects in aluminum and beryllium from free surface velocity measurements," in: Metallurgical Effects of High Strain Rates, New York–London (1973).
41. S. Cochrane and D. Banner, "Spall studies in uranium," J. Appl. Phys., 48, No. 7 (1977).